Relation of athermal Jamming and Random Organization

Master's Thesis Physics

by

Georg Thomas Christian Axmann

July 9, 2024

Friedrich-Alexander-Universität Erlangen-Nürnberg

Supervisor: Prof. Dr. Michael Schmiedeberg

Abstract: *The random close packing phenomenon has been studied as the densest absorbing states in models from the universality class of conserved directed percolation. So far, the dynamic implemented in such models always incorporated a random aspect. We implement numerically a fully deterministic absorbing state model of soft spheres, together with a modified, partly random version. For the deterministic model we find* $\phi_c = 0.6398(5),\ \beta = 0.88(2),\ \nu_{\parallel} = 1.29(6)$ *as a first result. We hypothesize that the deterministic model can be viewed as a limiting case of the modification and that the unified model resides in the conserved directed percolation universality class.*

Contents

1 Introduction **4**

2 Theoretical Background **6**

2.1 Athermal Jamming in dense sphere packings 6

2.2 Random Organization 7

2.3 Modifications to random organization 8

3 The approach and its technicalities **9**

3.1 Description of the Protocol 9

3.2 Calculating the overlap information 10

3.3 Detecting clusters 10

3.4 Dealing with percolating clusters 12

3.5 Calculating the center of mass and relocating the particles 13

3.6 Modification: The chopped case 14

4 Critical exponents of the percolating case **15**

4.1 Tuning the simulation parameters 15

4.2 Calculating critical exponents 18

5 Choosing the order parameter **22**

6 Contrasting to the "chopped" case **25**

7 Conclusion and Outlook **27**

1 Introduction

While the mathematically optimal volume fraction[i] of identical spheres has been proven [1] to be the crystalline fcc packing density with $\phi_c \approx 0.74$, the densest state reached when compressing spherical objects in the physical world, even at low friction, is a disordered arrangement.

In experiments—from the earliest studies [2, 3], where the geometrical structure were extracted by dissecting wax encased packings, to the tomographical analysis of hundreds of thousands of particles [4]—the maximal volume fraction reached is oftentimes only ~ 0.64, which is at 86% of the crystalline density. Computer simulations with frictionless spheres (e.g. [5, 6, 7]) customary confirm this maximal density.

Further research on the properties of such sphere packings—usually referred to as random close packed configurations—revealed that they are isostatic, isotropic [8] and have suppressed long range density fluctuations [9] (are hyperuniform).

In the process of finding a unifying description of various athermal "jamming" transitions[ii] (which are governed by mechanical quantities: density and stress [10]) with the glass transition of thermal matter, O'Hern et al. linked [7, 11] random close packing to the critical point J of the "jamming phase diagram" (cf. e.g. [12, 13]). They found that a system of soft spheres (point particles with a finite range repulsive potential) can no longer avoid overlaps if its density is increased past this point [7]. Put succinctly, the onset of overlapping in a soft sphere system was found to be the onset of jamming.

[i] **Note:** In this text the terms "volume fraction", "packing fraction" and "density" are used interchangeably. The concept meant is the quantity $\phi = \frac{4\pi}{3}(\frac{d}{2})^3 \frac{N}{V}$, where d is the particle diameter, N the particle count and V the total volume.

[ii] Examples: ground coffee jamming in a funnel until the funnel is hit, concrete only flows through a net if it contains too much water or is vibrated.

Random organization (RO) [14, 15] is a model that lends itself to the task of studying this onset of overlaps. In discrete time steps a configuration of spherical particles is evolved according to a simple relocation strategy, where particles that overlap with another particle (called active particles) are displaced at random. Thus, the configuration eventually settles at a constant fraction of active particles (activity).

This fraction might either be zero, so that the dynamic ceases or nonzero. Choosing the activity as the order parameter, the model has been found to be in the universality class of conserved directed percolation [16, 17] (referred to as manna class [18]). Furthermore, it has been shown to share the hyperuniformity property of random close packing [19].

The critical point of random organization however happens at a much lower density than the random close packing density thus, random organization has been modified to contain a deterministic component, so that overlaps are reduced more purposefully. Hereby, random organization based models could recreate jammed configurations [20] and rephrase random close packing as the densest absorbing states of a manna class absorbing state model [21, 22]. These models are reffered to as biased random organization (BRO).

This thesis aims to go a step further, and implements a fully deterministic soft sphere model.

First previous models are discussed in more detail and parameters associated with random close packing are described and compared to those models (chapter 2). Then the necessary modifications to construct the deterministic protocol are introduced (chapter 3). The main results are discussed in chapter 4, the choice of the order parameter used is discussed in chapter 5. Last, but not least, a modification of the protocol is discussed in chapter 6.

2 Theoretical Background

2.1 Athermal Jamming in dense sphere packings

In a continuous time limit or more precisely a limit of infinitesimal particle displacement, the protocols to be discussed can oftentimes be viewed as a minimization problem in an energy landscape where each particle with diameter σ contributes a pair potential of the form

$$V(r) = \begin{cases} \frac{\epsilon}{\alpha}\left(1 - \frac{r}{\sigma}\right)^{\alpha} & r < \sigma, \\ 0 & r \geq \sigma, \end{cases}$$

that is, overlaps are energetically unfavourable, but particles do not notice each other apart from overlaps (soft spheres). Even though this limit is not applicable for all protocols, it has merit to examine the properties of the minimum energy states of such a potential. The global minimum energy state corresponts to a metastable state, that looks similar to one in equilibrium, where internal stresses leading to regions with persisting overlaps have relaxed. At the right density the global mimimum is the crystalline fcc arrangement[iii].

In the protocols however, a state with an asymptotically stable nonzero fraction of overlapping particles–a state in a local minimum–is possible even for densities below the crystalline packing density. For instance Milz and Schmiedeberg find a nonzero amount of overlapping particles above a volume fraction of ~ 0.63 [20].

In the context of the energy landscape, the states generated by the protocols might correspond to local minima, reached by a highly irreversible thermodynamic transition where the system is abruptly reduced in temperature, "quenched", in a short period of time.

Numerically, these states can be explored [7, 11] by transitioning a randomly picked initial state to the nearest minimum in the energy landscape (e.g. conjugate gradient method). With enough initial states, statistical insight in the state properties of interest

[iii] The global minimum consists of all states without any overlaps.

can be gathered. It has been found that there are many similarities in these local minima. An interesting result is that the existence of overlaps in the quenched configurations depends on density with a critical packing fraction of 0.64 (in three dimensions) parting regimes with and without overlaps [7].

Of major importance is the result that, setting the packing fraction to its critical value, the mean number of touching partners per particle Z is equal to the isostatic value, which is obtained if the number of translational degrees of freedom for all particles and the number of interparticle contraints balance,

$$3N = \frac{NZ}{2} \qquad \Leftrightarrow \qquad Z = 6.$$

This means that at critical packing fraction, the configuration becomes mechanically stable. No particle can be moved without developing an overlap with a different particle. Fitting mechanical stability, simulations have shown that the configurations develop a bulk and shear modulus at and above critical density [7].

This process, where a system of discrete particles develops traits of a solid under compactification is referred to as athermal jamming [10].

2.2 Random Organization

A rather basic relocation protocol called random organization [14, 15] chooses to move particles that share an overlap with other particles (sometimes referred to as active particles, from here on) at random, e.g. with a displacement vector $\vec{r} = \tilde{\epsilon}\hat{r}$ where $\hat{r} \in S^2$, $\tilde{\epsilon} \in [0, \epsilon]$ uniformly, and ϵ is a parameter. Overlaps will eventually die out at low density, while densities above a critical density $\phi_c(\epsilon)$ lead to indefinite dynamics, where overlaps can never be avoided for all particles at the same time. At long times, the fraction of active particles approaches a steady value, the configuration becomes stationary and density fluctuations become depressed. Furthermore, the system becomes hyperuniform [19].

This can be seen to mark a nonequilibrium phase transition between the subcritical so called absorbing states, where the dynamic ceases at some point and the supercritical so called active states with a dynamical large time configuration that exhibits stationary properties. The critical density depends on the number of particles and on ϵ and approaches a well defined value (around 0.2 in three spatial dimensions) in a limit of low ϵ and high particle count. The time scale during which states evolve to a steady or an inactive configuration depends on the density of the system and diverges with a

critical exponent near the phase transition. Also the long time fraction of active particles depend on density, varying continuously from 0 at low densities to a nonzero value at higher densities, with a critical exponent near the phase transition. From the critical exponents, the model can be attributed to the universality class of conserved directed percolation [16] (often refered to as the Manna class [18]).

2.3 Modifications to random organization

The random organization model leads to a critical density much lower than the crystalline density. Random organization can been modified, to entail a deterministic component that helps moving particles away from each other more purposefully. An important consideration to be made when designing such a modification is the treatment of clusters of overlapping particles.

The biased random organization model [21, 22] for instance modifies random organization by identifying the center of mass of an a cluster of active particles to then move all particles directly away from the center of mass with a random amplitude. While doing so, only clusters within predefined regions are considered, overlaps to particles outside of a region are neglected. Another modification [20] randomly chooses a pair if multiple candidates are available but makes the relocation such that the particles touch (which would be completely deterministic, if there could never be more than two particles touching at the same time).

Both modifications arrive at a critical density of 0.64 and Manna universality, while also reproducing the hyperuniformity of random organization. The particle configurations show the properties known from athermal jamming.

While all previous implementations[iv] contained some kind of randomness, this thesis imposes a completely deterministic relocation protocol. This requests, that clusters of overlapping particles are left intact up to the extreme case of clusters rendered effectively infinite by means of the periodic boundary conditions. The relocation protocol is inspired by [20] and [21], it displaces particles relative to the center of mass. Since for such "infinite" clusters the center of mass is ill defined, they require special treatment in this protocol.

In a modified model, some randomness is reintroduced, by chopping the system into smaller parts based on a randomly moving grid, before the clusters search.

[iv] That the author is aware of.

3 The approach and its technicalities

In this chapter, we shall introduce the relocation strategy employed in this thesis and examine the technical realisation of the protocol.

3.1 Description of the Protocol

Given volume fraction ϕ, particle count N, maximum step count T and relocation parameter f (a small positive number) as parameters to the protocol, carry out these steps:

- As preliminary steps:
  - Calculate the particle diameter $d = \sqrt[3]{\frac{6\phi}{N\pi}}$.
  - Place each of the N particles at $(x, y, z) \in [0, 1]$ drawn from a uniform distribution.
- Repeat at most T times, the following steps:
  - The protocol stops, in case no active particles remain.
  - Otherwise, find clusters of overlapping particles, where overlaps respect boundary conditions (see below).
  - For each such cluster, find their center of mass $\vec{R}$ and move each particle in it from the current position $\vec{r}$ to $f \cdot (\vec{r} - \vec{R}) + \vec{R}$.
  - If the cluster percolates (see below), the center of mass calculation becomes ill defined. In that case, treat particles as inactive, based on a rudimentary connectedness ranking. Increase the number of ignored particles until the percolation property no longer applies.

3.2 Calculating the overlap information

In the unmodified protocol, particles located at $\vec{r}$ and $\vec{s}$ are considered overlapping if $\|\vec{r}-\vec{s}+\vec{\delta}\| < d$ for $\vec{\delta}$ equal to any of $\{(a,b,c) \mid a,\, b,\, c \in \{0,\pm 1\}\}$. This means they overlap with respect to three dimensional euclidean geometry modified to periodic boundary conditions in the unit cubic volume. Periodic boundary conditions imply, that opposing faces of the enclosing cube are essentially considered identified.

A modified version of the protocol, explained in 3.6, allows for some overlap information to be ignored, effectively chopping the system into smaller subvolumes before detecting the clusters.

There are $\binom{N}{2} = \mathcal{O}(N^2)$ pairs of particles, which means that computing performance would be impaired, if each pair would have to be checked individually. The implementation circumvents unnecessary comparisons, by employing a cell list. The enclosing volume is considered to consist of $n^3,\ n = \lfloor 1/d \rfloor$ equally sized cubic cells, and for each cell, a list of references to the particles it contains is maintained throughout the simulation. The size of the cells is $1/n \geq d$, ensuring, that only particles in neighboring cells can have an overlap. At the same time, particles in the same cell can still have a distance of more than d. When checking for particle overlaps, for each of the cells, pairs within itself and between itself and half of its neighbors [v] need to be checked. Since the number of comparisons for each cell only depends on the number of particles in the cell and in its neighbors cell, this brings the number of comparisons down to $\mathcal{O}(N)$.

3.3 Detecting clusters

Treating the overlap information as a graph, where vertices represent particles and edges represent the interparticle relation of overlapping, a cluster is defined as a connected component of the graph. In the implementation, the graph is represented by its adjacency matrix. Memory usage can be optimized here, since such a matrix, for a nondirected graph, unweighted graph, is symmetric, and only has entries equal to 0 or 1, where in this case, the majority of entries are 0 (the matrix is sparse).

[v] each cell can check the 9 cells below it, the 3 cells left of it and the 1 cell behind it, and consequently is checked by the 9 cells above, 3 cells to the right and 1 cell before it itself, warranting all pairs be checked

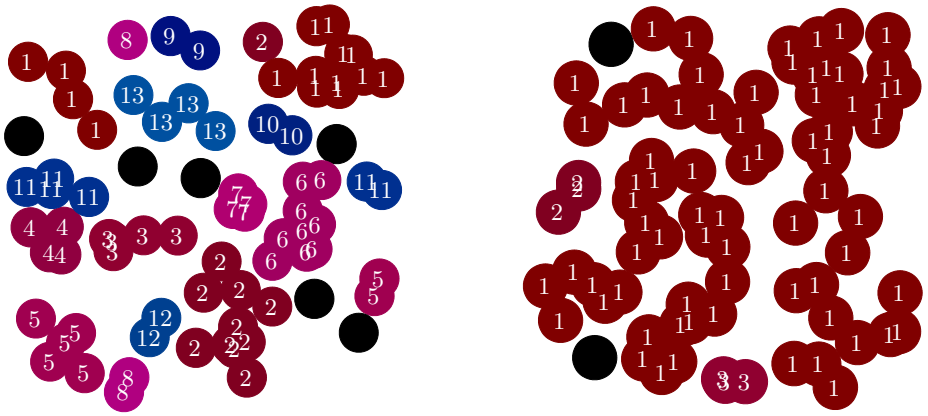

Figure 3.1: *Particles sorted into clusters of overlapping particles. Some clusters "wrap around" due to the imposed periodic boundary conditions. The cluster on the right percolates. Each particle is labeled by an arbitrary identifier for its cluster.*

The algorithm used to find connected components in the graph is a breadth first search (cf. e.g. [23]). Starting at an arbirary vertex, the search reaches any other vertex only, if it can reach it by visiting neighbors of vertices recursively. By this means, each vertex can be flagged to belong to a certain connected component. Figure 3.1 shows an examplary sorting in two dimensons.

Since it is necessary to iterate through the neighbors of a vertex it suggests itself to represent the adjacency matrix by a list where the i-th item is the list of indices of the neighbors of the i-th vertex. This representation ignores a possible optimization via the symmetric property of the adjacency matrix. Each edge would only need to be represented once, but since both of the vertices have all of their neighbors listed, it is represented twice. This is intentional, else the implementation would need to calculate the missing neighbors by effectively calculating a transpose of the matrix. The breadth first search has a time complexity of $\mathcal{O}(N)$, as the amount of neighbors for each vertex can be assumed to be $\mathcal{O}(1)$.

3.4 Dealing with percolating clusters

Having sorted all points into a cluster, the next step of the protocol is to go through each of the clusters, calculate their center of mass and then relocate all of its particles relative to that center of mass. Interpreting the employed periodic boundary conditions, it becomes possible for a cluster to overlap with its periodic repeat. If that happens, the cluster essentially fills all of space, the center of mass becomes ill defined and the cluster is said to percolate. The right side of figure 3.1 shows a percolating cluster in two dimensions.

In order to determine whether a cluster satisfies the percolation property, we first choose one of the three associated pairs of faces of the confining cube. Then we determine what subclusters the cluster would decompose to, if the periodicity orthogonal to these faces would be dropped, i.e. if edges in the overlapping graph would be dropped that correspond to pairs of particles overlapping across the pair of faces. The original cluster could only have percolated, if any of these subclusters connects both faces. If such a subcluster is found, it is searched for a pair of particles that would overlap if the opposing faces are identified again. If no such subcluster is found, the procedure is repeated for the other two pairs of faces.

If a cluster does indeed percolate, we choose to relocate the particles of some of its subclusters. The algorithm to determine these subclusters consists of the following steps.

- Weight the particles by their cumulative overlapping depth [vi].
- Ignore the particle with the least weight, that is, remove edges connecting it to other particles in the graph representing the overlap information.
- Calculate whether the removal of the adjacency information has caused the percolating cluster to split up.
- Calculate for each of the subclusters of the current cluster whether it is still percolating.
- Repeat these steps until the percolation property is no longer found in any subcluster.
- Apply the relocation strategy of finding the center of mass and relocating all particles belonging to the cluster relative to that center of mass to all new found subclusters.

[vi] for a particle at $\vec{r}$, this is $\sum_i (d - \|\vec{r} - \vec{r}_i\|)$, where the sum cycles through all particles overlapping with that particle

A percolating cluster and consequently also the time it takes to detect its subclusters is of size $\mathcal{O}(N)$. The number of particles to be ignored cannot realistically be assumed to be $\mathcal{O}(1)$, which brings the time complexity of the reduction algorithm to above $\mathcal{O}(N)$. This means that the approach might not be able to investigate at large enough N, to give statistically sound insight.

3.5 Calculating the center of mass and relocating the particles

Having found all active particles and the non-percolating clusters they belong to, the remainder of the step is to actually relocate the particles. This is done in three steps. In a first step, all particle coordinates are translated to $\mathbb{R}^3$ coordinates, so that particles that overlap by means of the periodic boundary condition overlap in flat space. In a second step, the center of mass $\vec{R}$ with respect to these coordinates is computed, the relocation

$$\vec{r} \quad \mapsto \quad f \cdot (\vec{r} - \vec{R}) + \vec{R}$$

is applied to each of the particles the cluster consists of, and in the third step, the coordinate is translated back to the unit volume again.

The translation to $\mathbb{R}^3$ coordinates happens through a breadth first search. For a particle located at $\vec{r} = (x, y, z)$, any newly visited overlapping particle located at $\vec{s} = (x', y', z')$ is moved

$$\vec{s} \quad \mapsto \quad \begin{pmatrix} x' \\ y' \\ z' \end{pmatrix} + \begin{pmatrix} \mathrm{rd}(x - x') \\ \mathrm{rd}(y - y') \\ \mathrm{rd}(z - z') \end{pmatrix}, \qquad \mathrm{rd}(x) \coloneqq \mathrm{sign}(x) \cdot \left\lfloor |x + \tfrac{1}{2}| \right\rfloor, \text{ (rounding)}$$

i.e. it is moved by a distance $\in \mathbb{Z}^3$, such that it overlaps with the particle at $\vec{r}$ with respect to the euclidean metric. By the time the breadth first search has finished, each particle thus overlaps in euclidean $\mathbb{R}^3$ with the particles it overlaps with according to the adjacency matrix.

The backtranslation happens by discarding the integer part:

$$\begin{pmatrix} x \\ y \\ z \end{pmatrix} \mapsto \begin{pmatrix} x - \lfloor x \rfloor \\ y - \lfloor y \rfloor \\ z - \lfloor z \rfloor \end{pmatrix}.$$

3.6 Modification: The chopped case

Other than the previosly mentioned modifications to the random organization model, the deterministic model does not artificially chop clusters of overlapping particles into smaller parts (of only $\mathcal{O}(2)$ particles per cluster). A modification to the deterministic model is introduced, in order to reintroduce and investigate on the influence of this feature. To this end, a new parameter C, is introduced. It controls the lengthscale of the chopping. In the limit of infinite C, the deterministic model should be recovered.

Changes to the relocation step

Before the coordinates of each particle are backtranslated, every particle is dislocated by the same random displacement vector. The vector is drawn from a uniform distribution in $[0,1]^3$, once each step. This modification would not have any effect on the original model.

Changes to the overlap information

Particles located at $\vec{r}$ and $\vec{s}$ are only considered to be overlapping, if

$$\lfloor M \cdot r_i \rfloor = \lfloor M \cdot s_i \rfloor \ , \quad \forall i \in \{1,2,3\} \ , \quad M = \max\left(1, \left\lfloor \frac{1}{Cd} \right\rfloor\right) .$$

This means the volume is considered to be chopped into M^3 parts of size $\frac{1}{M} \geq C \cdot d$, i.e. each part is of the size of at least C particles.

In order to distinguish the different dynamic protocols, the latter is referred to as the "chopped" case and the former as the "percolating" one.

4 Critical exponents of the percolating case

To examine the behavior of the protocol we analyse the properties of an order parameter as a function of time, where time is the product of the relocation parameter and the simulation step count. The order parameter chosen is the median[vii] of $\sigma := d - \|\vec{r} - \vec{s}\|$[viii] for all distinct overlapping pairs located at $\vec{r}$ and $\vec{s}$, referred to as the median overlap. In all following graphs, the overlap is measured in units where $d = 2$.

As a first step simulation parameters are varied to explore finite size effects.

4.1 Tuning the simulation parameters

From fig. 4.1 we see that the median overlap becomes independent from the relocation parameter f once this parameter becomes smaller than a certain threshold. For these simulations $\phi = 0.62$ is chosen as the density parameter near the expected critical density. While for $f < 0.005$ the overlap approaches zero at $t \sim 300$[ix], for larger f, the overlap approaches a constant, nonzero value that varies with f.

This means that for larger f the system enters supercritical behavior (overlaps never extinct) at lower densities and the critical density would be underestimated when using an f parameter within this range. At larger f, particles are moved further distances, which can make it impossible for some overlaps to be resolved.

The relocation parameter cannot be reduced indefinitely, however, as the required step count to reach a certain time point is inversely proportional to f . Thus, we choose $f = 10^{-3}$ for future calculations, as this value is well within the regime where simulation outcomes behave coherent, but still allows for some computational performance.

[vii] For the percentile definition in use see chapter 5

[viii] $d = \sqrt[3]{\frac{6\phi}{N\pi}}$, particle diameter

[ix] roughly halfway between 100 and 1000 on a logarithmic scale

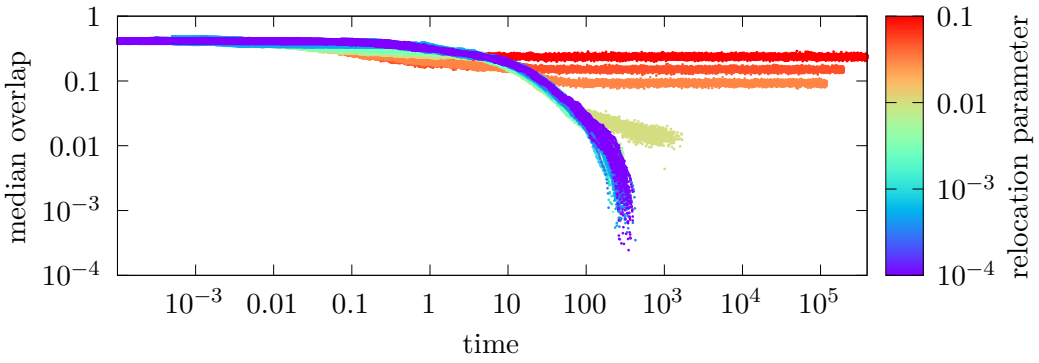

Figure 4.1: *Median overlap as a function of time for various relocation parameters. For each relocation parameter, 16 different random starting configurations are plotted. The system has 300 particles and a density of* 0.62*.*

In figure 4.2 we explore the influence of the particle count N on the time dependency of the overlap. For three different density values below the expected critical density and one value above it, we show curves for eleven different N. While the behavior is erratic for $N = \mathcal{O}(10)$, the behavior for $N \gtrsim 50$ already shows much similarity to the $N = 10^3$ case. At $N \geq 350$, the behavior within 16 runs is already mostly consistent.

For $N \geq 50$ dynamics can behave supercritical in the case the $N = 1000$ case behaves subcritical. Thus, the critical density would be underestimated if N is chosen too low. The frequency of these aberrations increase if the density is closer to the expected critical value. While it is necessary to choose density values close to the expected critical density to examine the critical behavior, the outcome of simulations at or very close to this density can therefore be trusted less.

This means that the curves near to the critical density can be improved in accuracy by either decreasing f or increasing N . This apparent correlated influence of f and N on the is plausible: the amount of particle diameters a particle is moved within a step is $\sim \frac{f}{N^{1/3}}$. Within a certain range, the larger this number, the higher the probability that a new overlap is created by the relocation.

To choose a good N, f set, two features of the $\sigma(t)$ curve that are most important for the critical exponent analysis in the next section:

$\phi < \phi_c$**:** The time point τ at which the curve reaches $\sigma = 0$ (and by definition would stay at 0 indefinitely after).

$\phi > \phi_c$**:** The overlap value at large times σ_∞.

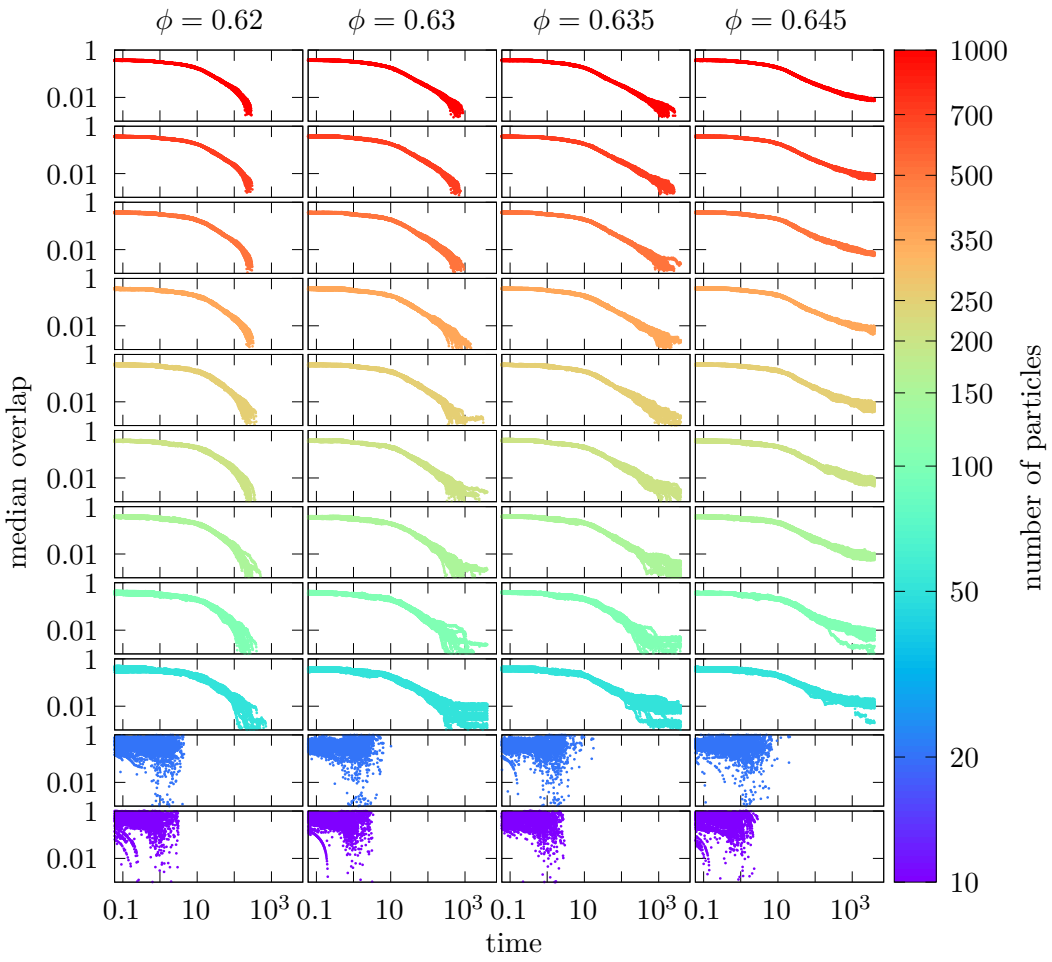

Figure 4.2: *Median overlap as a function of time for various numbers of particles and densities. For each pair of density and particle number 16 different random starting configuration are plotted. The relocation parameter is* 10^{-3} *in all cases.*

While the value of τ depends very little on N, its spread does. If the density is restricted to $\phi < 0.635$, for the given data at $f = 10^{-3}$, the spread is acceptable if $N > 350$.

The given data indicates that σ_∞ would need a much larger maximal step count. The value does not depend much on N.

Considering all this, we choose $N = 400$ for future calculations and refrain from calculations at density values inside of the interval $(0.635, 0.645)$.

4.2 Calculating critical exponents

To calculate the critical exponents we run multiple simulations through a range of densities around 0.64 at $N = 400$ and $f = 0.001$. For each density, six curves for different random starting configurations are simulated. We compare the calculated critical exponents to the BRO critical exponents [21, 22]. The exponents $\nu_\parallel$ and β are also compared to the exponents found for conserved directed percolation in 2D and 3D systems as shown in [20]. This comparation is shown in table 4.1.

Figure 4.3 shows the averaged curves for all simulated densities within the range $0.4 \leq \phi \leq 0.75$. In order to extrapolate the critical behavior of the order parameter depending on time $\sigma(t) \sim t^{-\xi}$ we fit this function to the curves at the two bordering densities and calculate the geometric mean

$$\sigma(t; \phi_c) = \sqrt{\sigma(t; \phi_c - \epsilon) \cdot \sigma(t; \phi_c + \epsilon)}.$$

The resulting ξ value compares well with the BRO value (cf. table 4.1).

$\sigma_\infty(\phi) \sim (\phi - \phi_c)^\beta$ is calculated by averaging the last 10 time units (corresponding to 10^4 simulation steps) for $0.64 \leq \phi \leq 0.7$. The outcome then is averaged within the density and the standard deviation of this average is treated as uncertainty for the fit. The data is shown in figure 4.4. The calculated critical exponent β barely agrees with 3D Manna value. The critical density $\phi_c = 0.6396(5)$ agrees excellently with the expected critical density (cf. table 4.1).

The slight discrepancy of the fitted β to the Manna value is likely due to undersampling. The fit takes place at 2 degrees of freedom, as only the longest running simulations have been used, which are computationally quite expensive. It would also be important to sample closer to the critical density. For this to be possible the simulation parameters would need to be recalibrated.

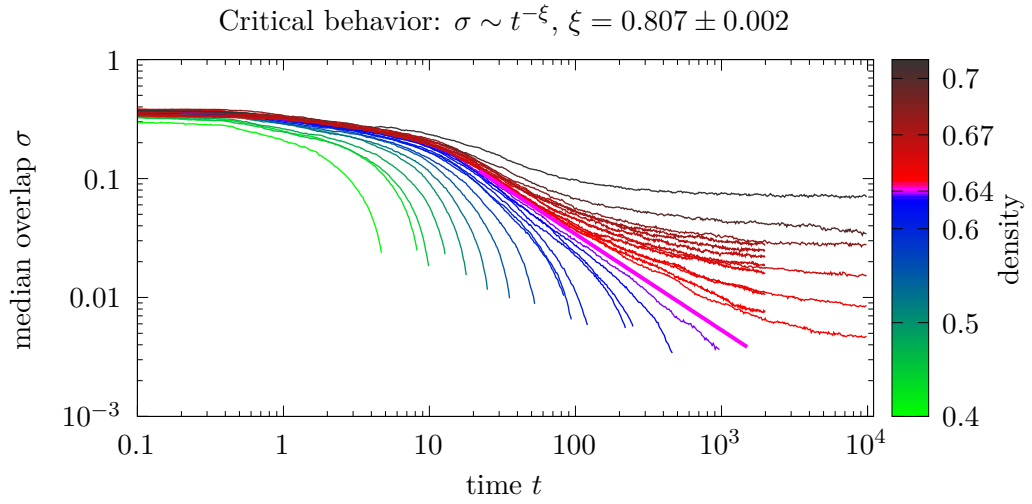

Figure 4.3: *Median overlap as a function of time for various densities. The relocation parameter is* 0.001 *and the particle count is* 400*. For each density, the time dependency is averaged for six random starting configurations. Also shown an extrapolation to criticality.*

Alternative to measuring σ_∞ by an average of σ at large t values, σ_∞ could be extrapolated by fitting an exponential decay

$$\sigma(t) = \sigma_\infty + \mathcal{O}\left(\exp\left(\frac{-t}{\bar{\tau}(\phi)}\right)\right),$$

possibly allowing for shorter simulation duration.

This would also allow for an alternative calculation for $\nu_\parallel$, by interpreting $\bar{\tau}(\phi)$ as a relaxation timescale of the system that behaves

$$\bar{\tau}(\phi) \sim (\phi - \phi_c)^{-\nu_\parallel}.$$

As $\tau(\phi) \sim (\phi_c - \phi)^{-\nu_\parallel}$, we define the first point in time where $\sigma(t)$ becomes zero. This time point is extracted for all densities between 0.6 and 0.64 and averaged within the density, while the standard deviation of this average is treated as uncertainty for the fit. The data is shown in figure 4.5. While $\phi_c = 0.6399(5)$ agrees with the value from the previous fit, $\nu_\parallel$ fits does not fit the 3D, but the 2D Manna value (cf. table 4.1).

The discrepancy in this fit is likely due to the large uncertainty in determining the value of τ near the critical density. Figure 4.5 shows that the relative error in τ increases quite a bit (while not exceeding 1) when the critical density is approached. Improving the accuracy of the τ estimate, can be done by sampling more curves at the same density, and by decreasing f.

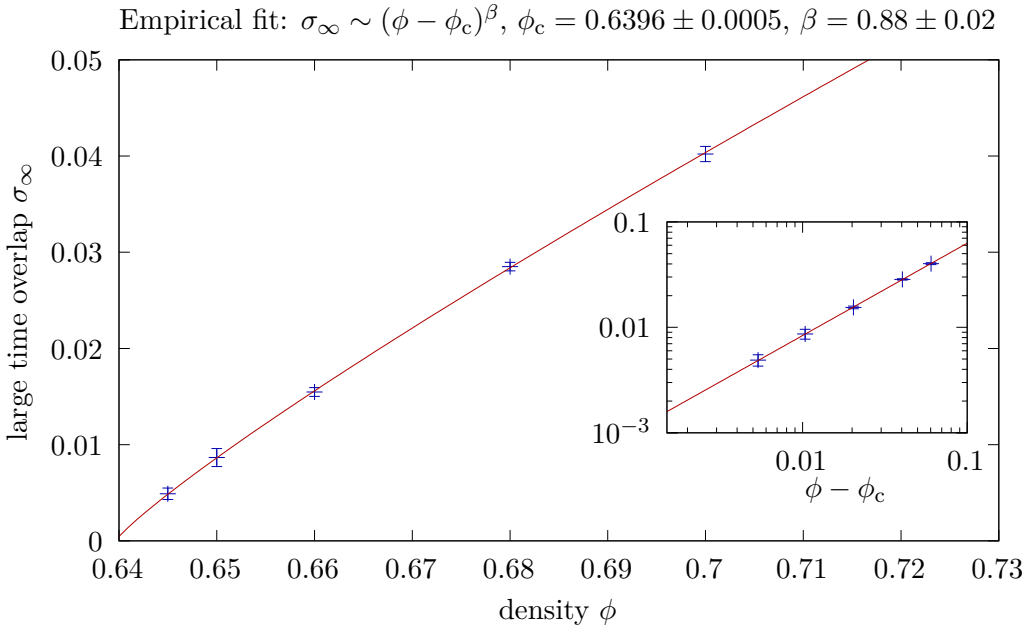

Figure 4.4: *Median overlap in a large time limit σ_∞ with an empirical power law fit. The data is averaged for 6 random starting configurations, the error bars indicate the standard deviation for this average. The relocation parameter is 10^{-3}, particle count is 400. The density is constrained below 0.71 to capture near critical behavior. For densities below 0.64, the limit median overlap is 0 per definition, therefore this data is excluded.*

Put together, the model shows a continous dynamic phase transition at a critical density that agrees with the random close packing density in three dimensions. The universality class could not be fully determined.

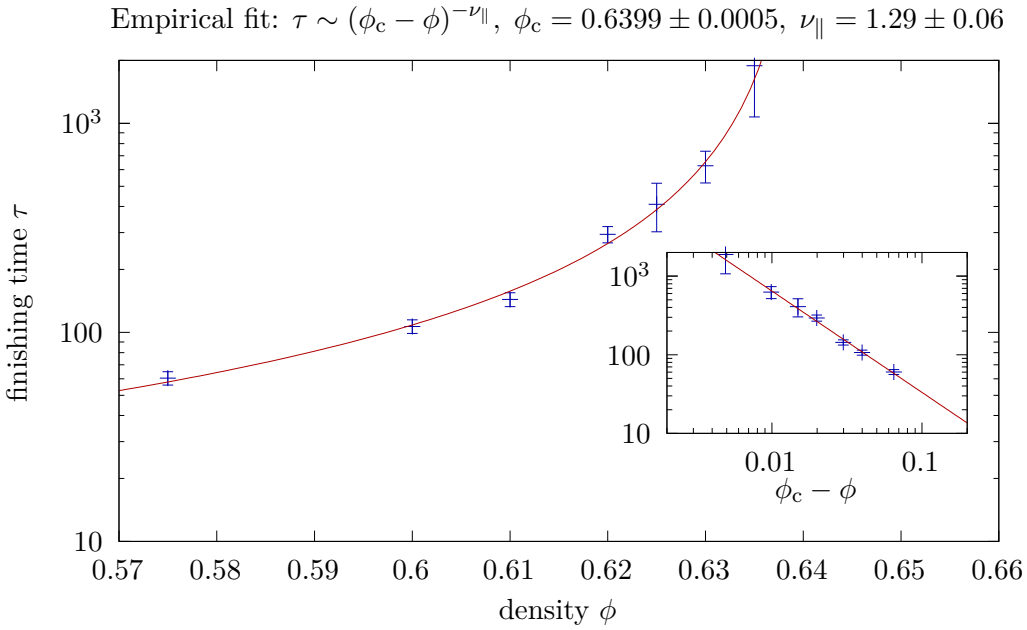

Figure 4.5: *Simulation duration τ as a function of density with an empirical power law fit. The data is averaged for 6 random starting configurations, the error bars indicate the standard deviation for this average. The relocation parameter is 10^{-3}, particle count is 400. The density is constrained to above 0.57 to capture near critical behavior. For densities above 0.64 we found $\frac{\tau}{f} = T$ independent of T, therefore this data is excluded.*

Table 4.1: *Critical behavior of the percolating model in this thesis compared to literature values. ϕ_c is given as a mean from the two different ways it was estimated. The numbers for the BRO case are taken from [21, 22], the Manna critical exponents are taken from [20]. ξ, the power law approach to zero of the order parameter at criticality is missing in [20]. The values for $\nu_\parallel$ and β are given without uncertainty in [21].*

	$\nu_\parallel$	β	ξ	ϕ_c
Thesis	1.29(6)	0.88(2)	0.802(1)	0.6398(4)
BRO	1.08	0.84	0.7(1)	3D: 0.640(1) 2D: 0.905(2)
Manna 3D	1.08(3)	0.84(2)		
Manna 2D	1.23(3)	0.639(9)		

5 Choosing the order parameter

Past random organization modifications (cf. e.g. [20] and [21, 22]) customary chose the fraction of active particles[x] as the order parameter. The thesis, however, chooses the median overlap.

Figure 5.1 shows the activity as a function of time for $0.4 \leq \phi \leq 0.75$, together with $\tau(\phi)$ for $\phi < \phi_c$. The behavior of the activity as a function of time generally shows a (roughly) monotonic increase towards 1 followed by a monotonic decrease, either towards zero (for $\phi < \phi_c$) or towards a nonzero constant(for $\phi > \phi_c$). Quite clearly, $\tau(\phi)$, if defined as the time point where the activity for a given ϕ reaches 0 for the first time, could be extracted from this data as well.

The equivalent of $\sigma_\infty(\phi)$ for $\phi > \phi_c$, i.e. the activity at large times, for the present data would however be quite imprecise. To improve accuracy, further investigation with a larger particle count and at least one order of magnitudes higher maximum step count would be necessary. Having established in the previous chapter that the median overlap behaves more consistent, we are presented with a natural choice.

Additionally, Figure 5.2 shows statistics of the overlap at each time step for a representative simulation which was done at $N = 600$, $f = 10^{-3}$ and $\phi = 0.6$. The statistical quantities shown are the quartiles, an outlier range of 1.5×IQR together with the amount of outliers. Also shown is the activity.

The percentile definition used was

$$\mathcal{P}(p; \underline{x}) = x_i + (p - \tfrac{i}{n}) \cdot n \cdot (x_{i+1} - x_i) \ , \qquad i = \min(n-1, \lfloor np \rfloor),$$

where $\underline{x} = (x_0, \ldots, x_n)$ is a sorted list of the instances of the quantity the percentile is to be computed for. For instance $\mathcal{P}(0; \underline{\sigma}) = \sigma_0$ and $\mathcal{P}(1; \underline{\sigma}) = \sigma_n$ are minimum and maximum overlap, while $\mathcal{P}(\frac{1}{2}; \underline{\sigma})$ is the regular median, i.e.

$$\mathcal{P}(\tfrac{1}{2}; \underline{\sigma}) = \begin{cases} \sigma_i & n \text{ even}, \qquad i = \lfloor \frac{n}{2} \rfloor \\ \frac{\sigma_{i+1} + \sigma_i}{2} & \text{else.} \end{cases}$$

[x] that is, particles that overlap with at least one other particle

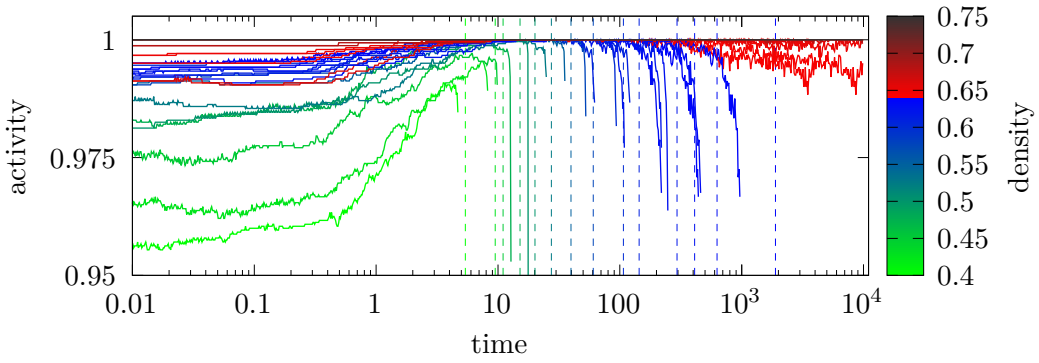

Figure 5.1: *Activity (fraction of active particles) as a function of time for various densities. The relocation parameter is* 10^{-3}*, the particle number is* 400*. The data shown is the average over 6 simulations per density value. The dashed lines indicate* $\tau(\phi)$ *if it exists.*

We see that there are a minimum of roughly 5% outliers throughout the whole simulation. Hence, the median overlap instead of the mean overlap as the order parameter is favourable. Since the activity is high ($> 90\%$ until very shortly before the simulation ends), the overlap is quite well defined statistically.

Moreover the range of the overlap values narrow at large times, indicating qualitatively the formation of uniform interparticle distances.

Figure 5.2 also highlights that the maximum overlap shows an exponential dependency on the step count $\frac{t}{f}$ until a certain point in time. This is a finite size effect: The largest overlap is due to a specific pair of particles, that continues to be the closest pair until a certain time.

With each step the protocol takes, the distance of these two particles is multiplied by $1 + f$. As a result their distance depends exponentially on time, $d - \max(\sigma_i) \sim (1 + f)^{\frac{t}{f}}$ (cf. section 3.5). The pair continues to be the closest pair only until the dynamic of the system starts to produce overlaps of the same size. In fact, fitting the exponential law to curves corresponding to different initial states shows a strong dependency of the proportionality factor of the initial state.

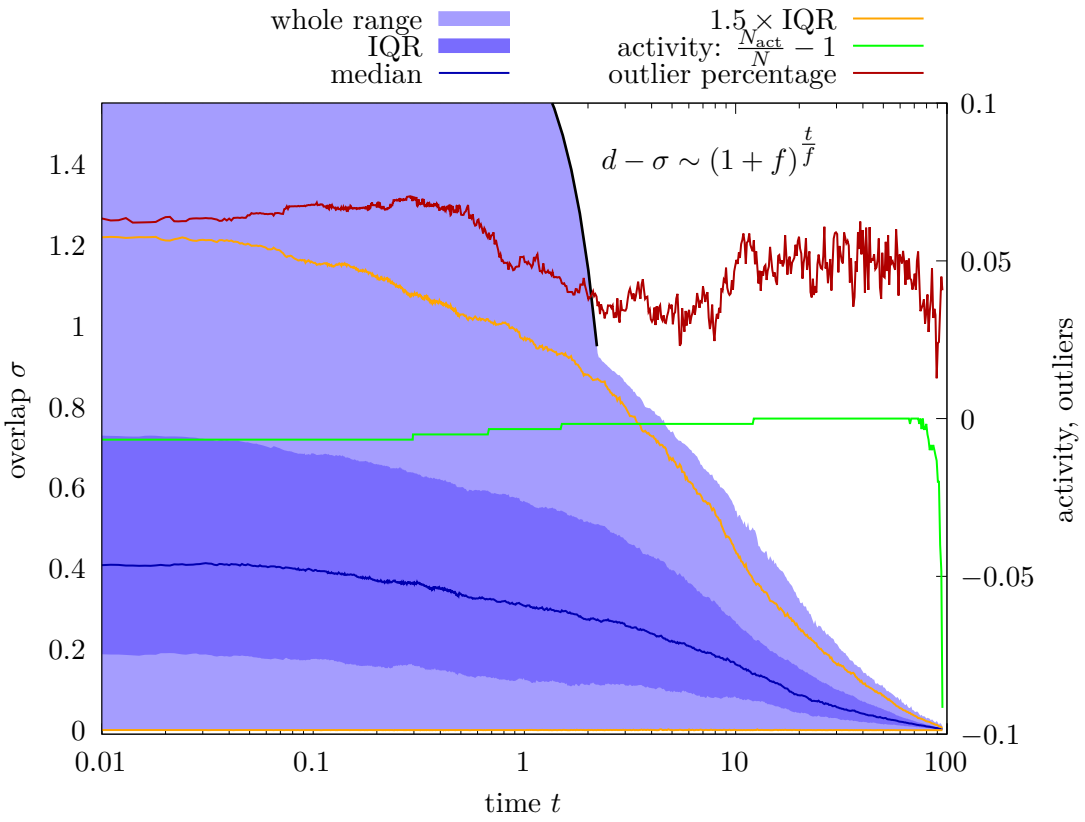

Figure 5.2: *Quartiles for the overlap between active particles as a function of time. The relocation parameter is* 10^{-3} *the particle number is* 600 *and the density is* 0.6*. Also shown are the fraction of active particles, an outlier range of* $1.5 \times$ IQR *and the fraction of active pairs that qualify as outliers. The labeled fit of the overlap maximum continues to fit until* $t = f$*, the rest of the data is merely cut out for visibility.*

6 Contrasting to the “chopped” case

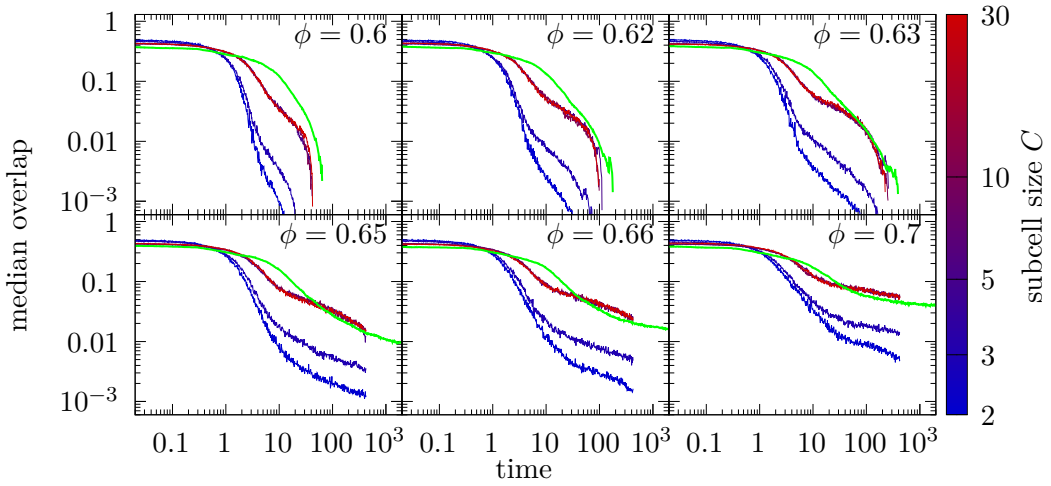

Figure 6.1: *Median overlap as a function of time, in the chopped case for various C and various densities. The relocation parameter is 10^{-4}, the particle number is 10^3. For each pair of parameters ϕ and C, 4 different random initial configurations are averaged. Also shown (green) is the data for the unmodified model.*

We now examine the modified “chopped” case, which reintroduces some randomness to the model by deliberately rejecting overlaps based on a randomly moving grid. Figure 6.1 shows the median overlap for various C, ϕ pairs. Since the computation efficiency is largely dominated by the cluster sizes and is heavily reduced if a percolating cluster is split up, the modified model computes much faster. It is however also quite susceptible to finite size effects, which is why $f = 10^{-4}$ and $N = 10^3$ were chosen.

The large C behavior quickly becomes consistent with the unmodified case, as would be expected. Qualitatively, low C curves show the same ϕ dependency as the percolating case curves, allowing to assume that a low C “chopped” model produces the same critical exponents.

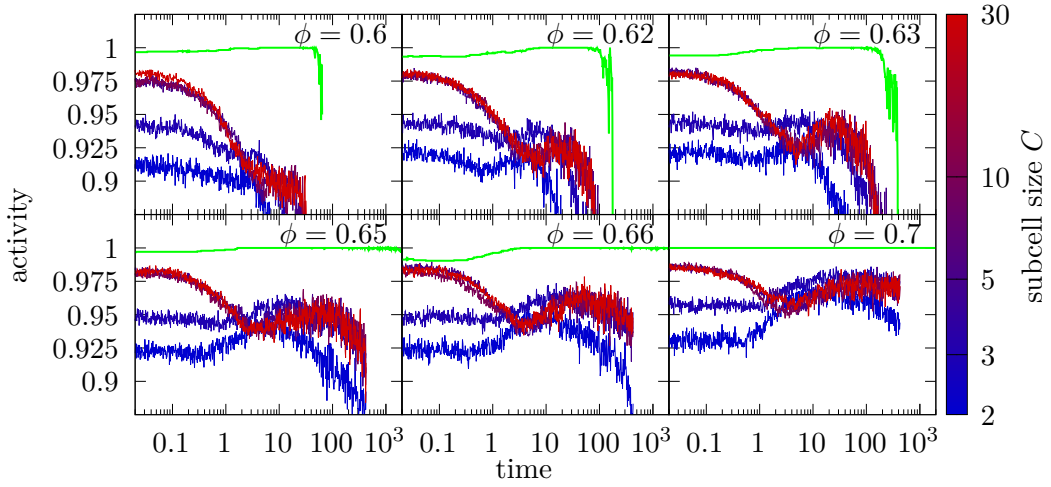

Figure 6.2: *Fraction of active particles as function of time, in the chopped case for various C and various densities. The relocation parameter is 10^{-4}, the particle number is 10^3. For each pair of parameters ϕ and C, 4 different random initial configurations are averaged. Also shown (green) is the data for the unmodified model.*

While the median overlap data limits towards the percolating case, the activity does not necessarily follow. Figure 6.2 shows the activity for various C, ϕ pairs at $f = 10^{-4}$, $N = 10^3$ together with the percolating case data for $f = 10^{-3}$, $N = 400$. It remains unclear whether this trend is a finite size effect. To resolve this, more tests need to be executed, especially at smaller f and much larger maximal time.

7 Conclusion and Outlook

The thesis implemented an absorbing state model with a completely deterministic dynamic. It was able to show that the critical point happens at a packing fraction of ≈ 0.64. The critical behavior could be characterized by three critical exponents. The universality class could not be fully determined. However, first results indicate, that this class is the Manna class.

A modification of the model was implemented, where the dynamic was made partly random by introducing an artificial length scale. There are grounds for the supposition, that in limiting the length scale towards large values, the modified version recovers the deterministic model. In order to prove this, the large time limit remains to be treated with more detail.

Furthermore, inspecting the physical properties of the particle configurations at criticality would allow to identify whether the densest absorbing states of the model are jammed configurations. Testing should be done for hyperuniformity, isotropy, isostaticity and a power law decay of interparticle gaps [8, 9].

Additional modifications of the model could lead to a better understanding of the influence of randomness on the phase transition and the configuration properties.

Lastly, the presence of a deterministic absorbing state manna class model could help to calculate an exact value of ϕ_c.

Bibliography

[1] Thomas Hales et al. "A formal proof of the Kepler conjecture". In: *Forum of mathematics, Pi*. Vol. 5. Cambridge University Press. 2017, e2.

[2] J D Bernal. "Co-ordination of randomly packed spheres". In: *Nature* 188 (1960), pp. 42–43.

[3] G David Scott. "Packing of spheres: packing of equal spheres". In: *Nature* 188.4754 (1960), pp. 908–909.

[4] Tomaso Aste, Mohammad Saadatfar, and TJ Senden. "Geometrical structure of disordered sphere packings". In: *Physical Review E—Statistical, Nonlinear, and Soft Matter Physics* 71.6 (2005), p. 061302.

[5] Boris D Lubachevsky, Frank H Stillinger, and Elliot N Pinson. "Disks vs. spheres: Contrasting properties of random packings". In: *Journal of Statistical Physics* 64 (1991), pp. 501–524.

[6] Alexander Z Zinchenko. "Algorithm for random close packing of spheres with periodic boundary conditions". In: *Journal of Computational Physics* 114.2 (1994), pp. 298–307.

[7] Corey S O'Hern et al. "Jamming at zero temperature and zero applied stress: The epitome of disorder". In: *Physical Review E* 68.1 (2003), p. 011306.

[8] Patrick Charbonneau et al. "Universal microstructure and mechanical stability of jammed packings". In: *Physical review letters* 109.20 (2012), p. 205501.

[9] Aleksandar Donev, Frank H Stillinger, and Salvatore Torquato. "Unexpected density fluctuations in jammed disordered sphere packings". In: *Physical review letters* 95.9 (2005), p. 090604.

[10] Ada Altieri. *The jamming transition*. Springer, 2019.

[11] Corey S O'Hern et al. "Random packings of frictionless particles". In: *Physical Review Letters* 88.7 (2002), p. 075507.

[12] Andrea J Liu and Sidney R Nagel. "Jamming is not just cool any more". In: *Nature* 396.6706 (1998), pp. 21–22.

[13] Thomas K Haxton, Michael Schmiedeberg, and Andrea J Liu. "Universal jamming phase diagram in the hard-sphere limit". In: *Physical Review E—Statistical, Nonlinear, and Soft Matter Physics* 83.3 (2011), p. 031503.

[14] David J Pine et al. "Chaos and threshold for irreversibility in sheared suspensions". In: *Nature* 438.7070 (2005), pp. 997–1000.

[15] Laurent Corte et al. "Random organization in periodically driven systems". In: *Nature Physics* 4.5 (2008), pp. 420–424.

[16] Gautam I Menon and Sriram Ramaswamy. "Universality class of the reversible-irreversible transition in sheared suspensions". In: *Physical Review E—Statistical, Nonlinear, and Soft Matter Physics* 79.6 (2009), p. 061108.

[17] Sven Lübeck. "Universal scaling behavior of non-equilibrium phase transitions". In: *International Journal of Modern Physics B* 18.31n32 (2004), pp. 3977–4118.

[18] Subhrangshu Sekhar Manna. "Two-state model of self-organized criticality". In: *Journal of Physics A: Mathematical and General* 24.7 (1991), p. L363.

[19] Daniel Hexner and Dov Levine. "Hyperuniformity of critical absorbing states". In: *Physical review letters* 114.11 (2015), p. 110602.

[20] Lars Milz and Michael Schmiedeberg. "Connecting the random organization transition and jamming within a unifying model system". In: *Physical Review E* 88.6 (2013), p. 062308.

[21] Sam Wilken et al. "Random close packing as a dynamical phase transition". In: *Physical review letters* 127.3 (2021), p. 038002.

[22] Sam Wilken et al. "Dynamical approach to the jamming problem". In: *Physical review letters* 131.23 (2023), p. 238202.

[23] Steven S Skiena. *The algorithm design manual*. Vol. 2. Springer, 1998.

Eigenständigkeitserklärung

Hiermit versichere ich, dass ich die vorliegende Masterarbeit selbständig verfasst habe. Ich versichere, dass ich keine anderen als die angegebenen Quellen benutzt und alle wörtlich oder sinngemäß aus anderen Werken übernommenen Aussagen als solche gekennzeichnet habe, und dass die eingereichte Arbeit weder vollständig noch in wesentlichen Teilen Gegenstand eines anderen Prüfungsverfahren gewesen ist.

Nürnberg, den 9. Juli 2024 **Thomas Axmann**